Supporting information for:

Amphiphilic phospholipid-based riboflavin derivatives for targeting nanomedicines

Nataliia Beztsinna[1], Yoannna.Tsvetkova[2], Matthias Bartneck[3], Twan Lammers[2], Fabian Kiessling[2], Isabelle Bestel[1]

[1] MMBE team, UMR 5248 CBMN, Bordeaux University, Pessac, France
[2] Experimental Molecular Imaging, RWTH Aachen University Clinic, Aachen, Germany
[3] Gastroenterology and Metabolic Disorders, RWTH Aachen University Clinic, Aachen, Germany

Table of contents

NMR spectra

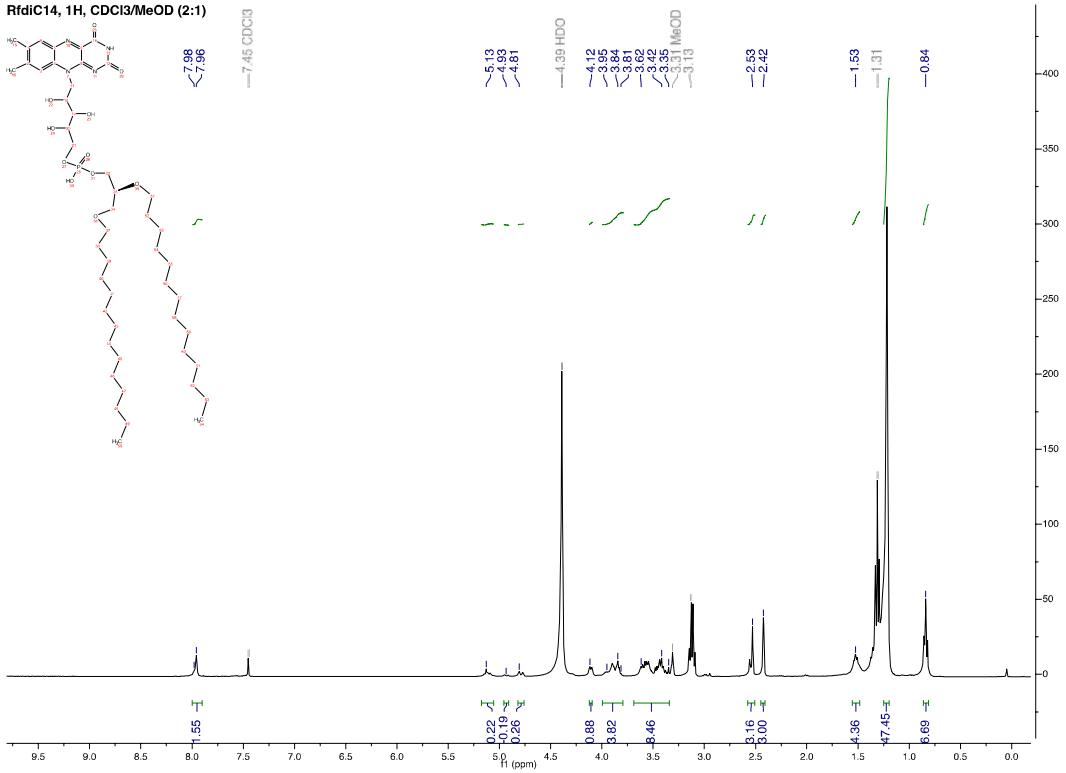

Figure S1. ^{1}H-NMR spectrum of RfdiC14 (compound **10**).

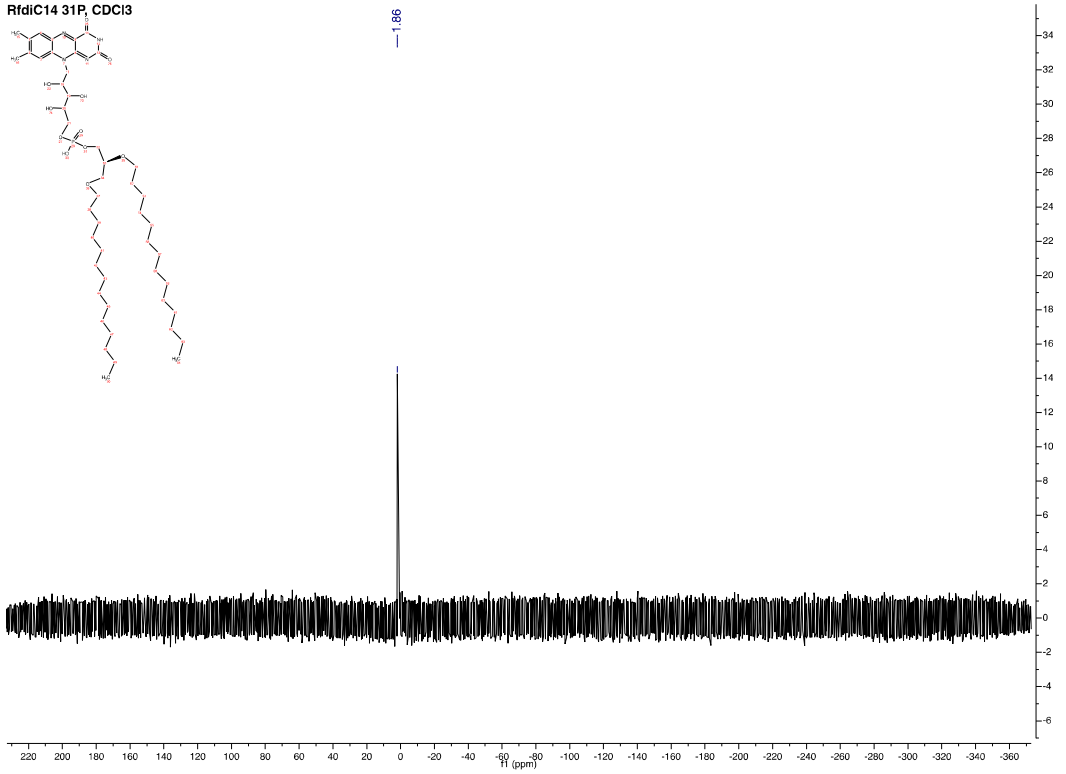

Figure S2. ^{31}P-NMR spectrum of RfdiC14 (compound **10**).

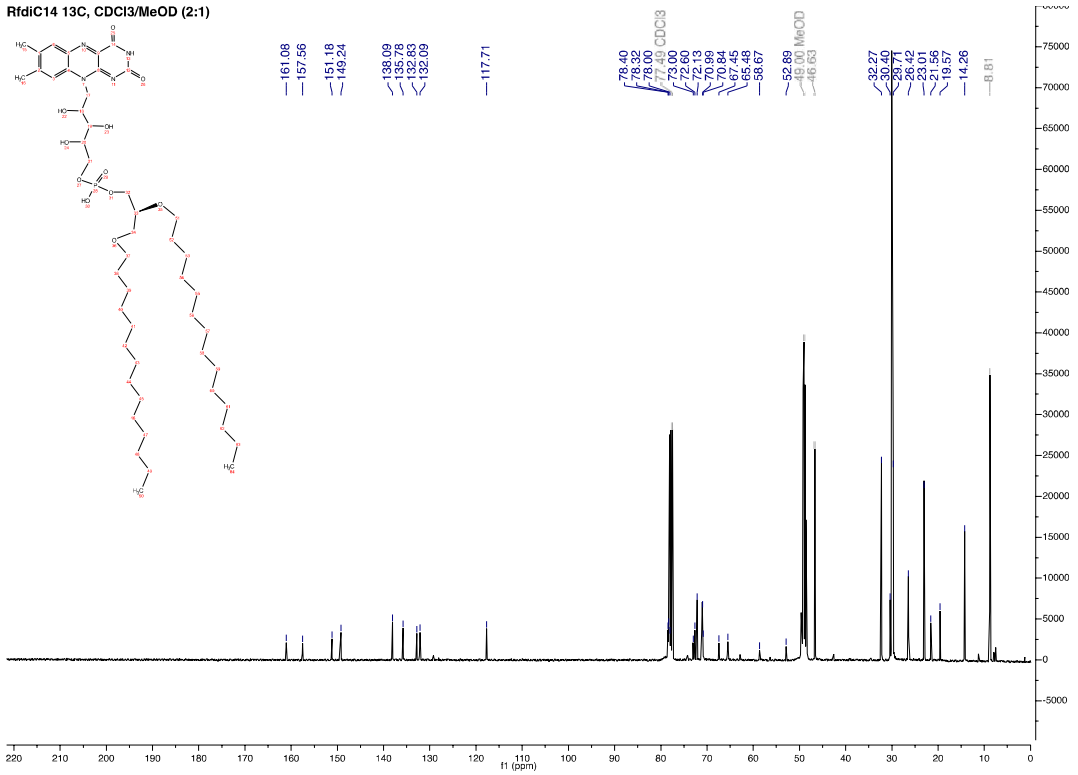

Figure S3. ^{13}C-NMR spectrum of RfdiC14 (compound **10**).

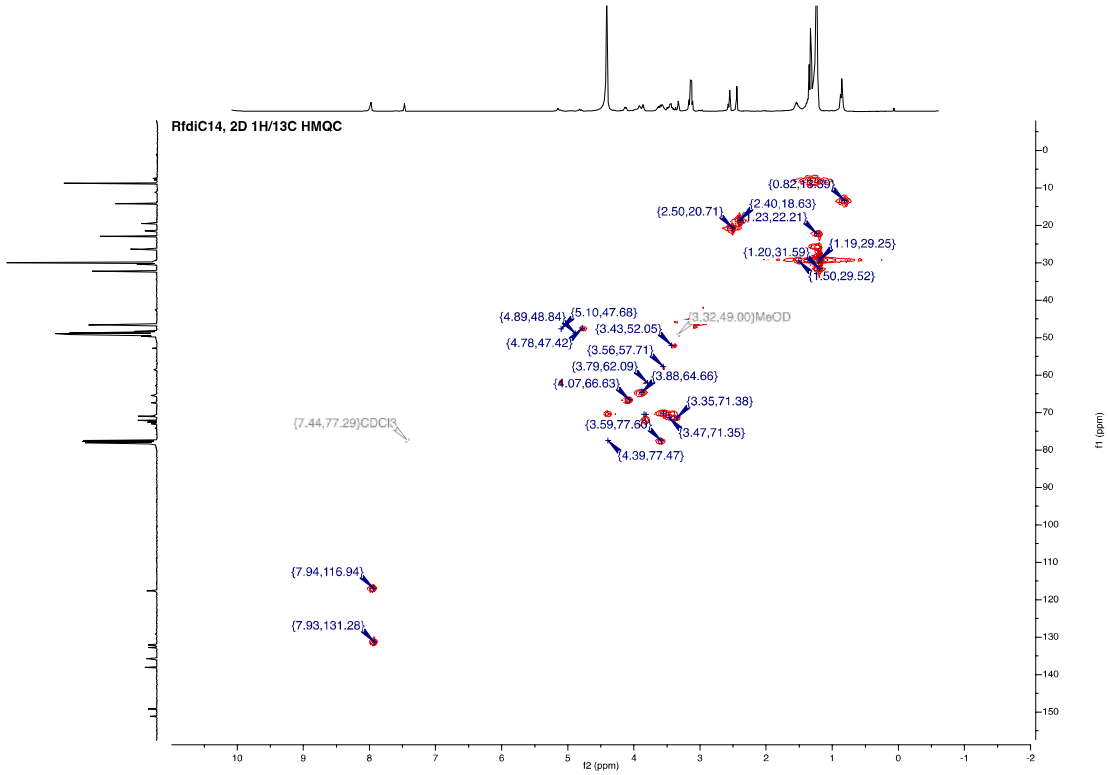

Figure S4. HMQC, 2D-NMR spectrum of RfdiC14 (compound **10**).

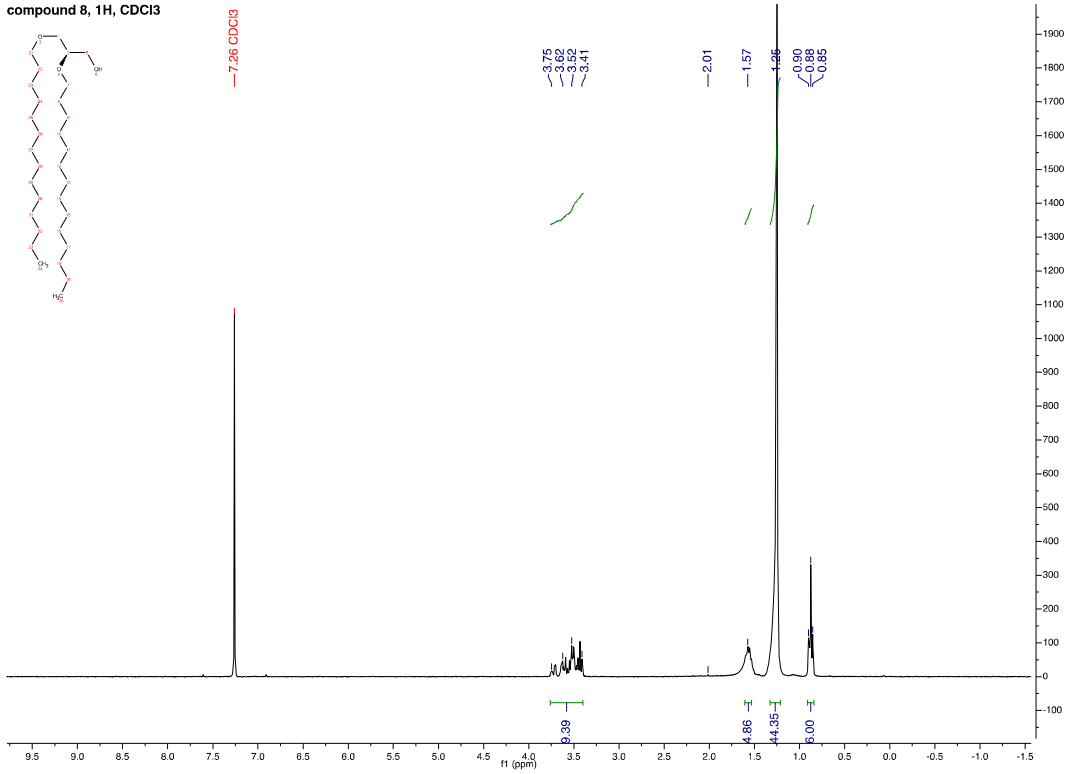

Figure S5. ^{1}H NMR spectrum of compound **8.**

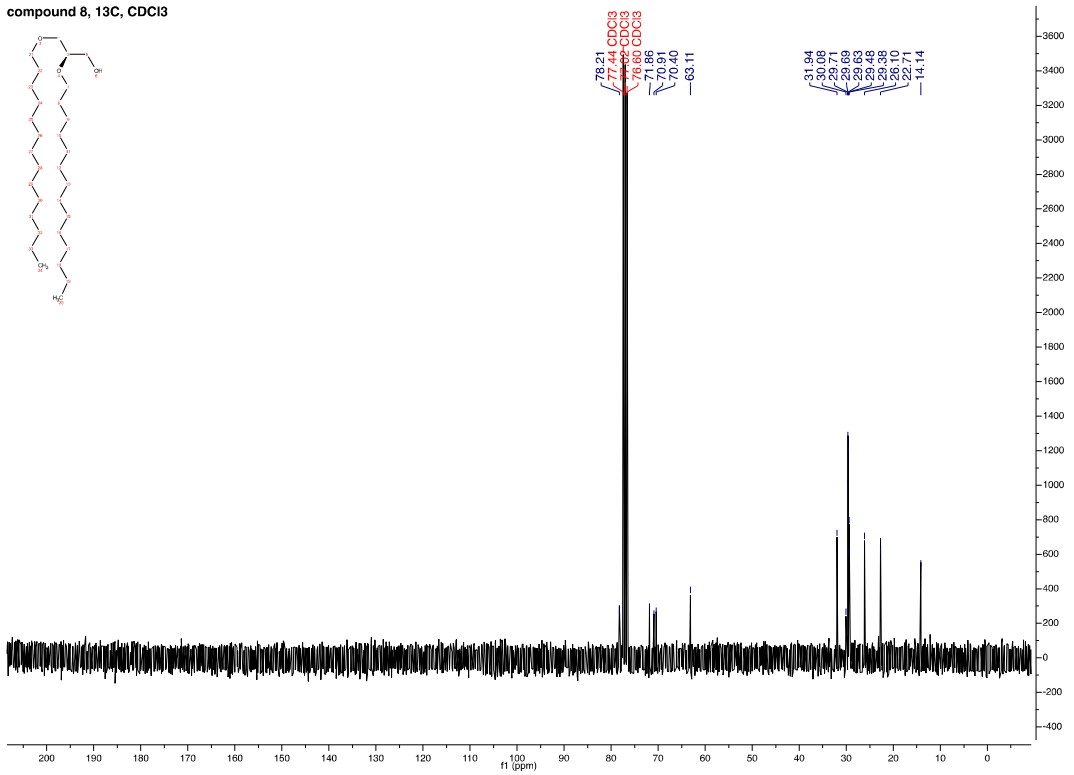

Figure S6. ^{13}C NMR spectrum of compound **8.**

ESI-MS spectra

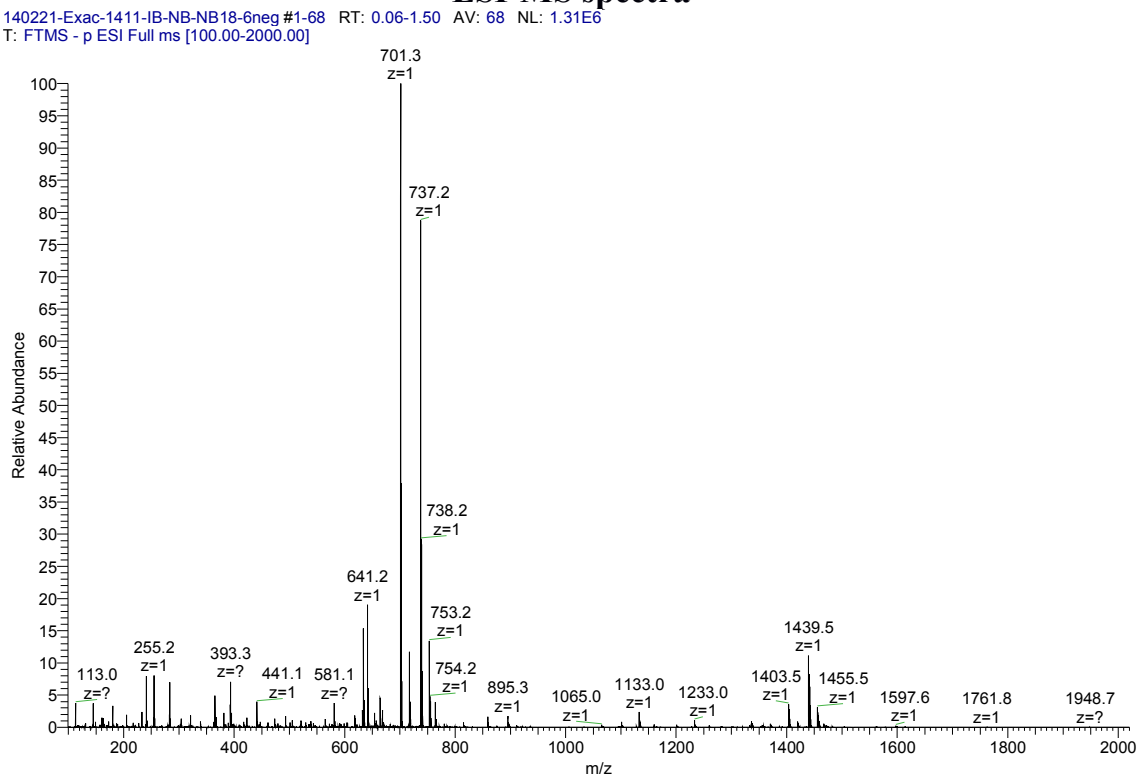

Figure S7. ESI-MS spectrum of compound **4.**

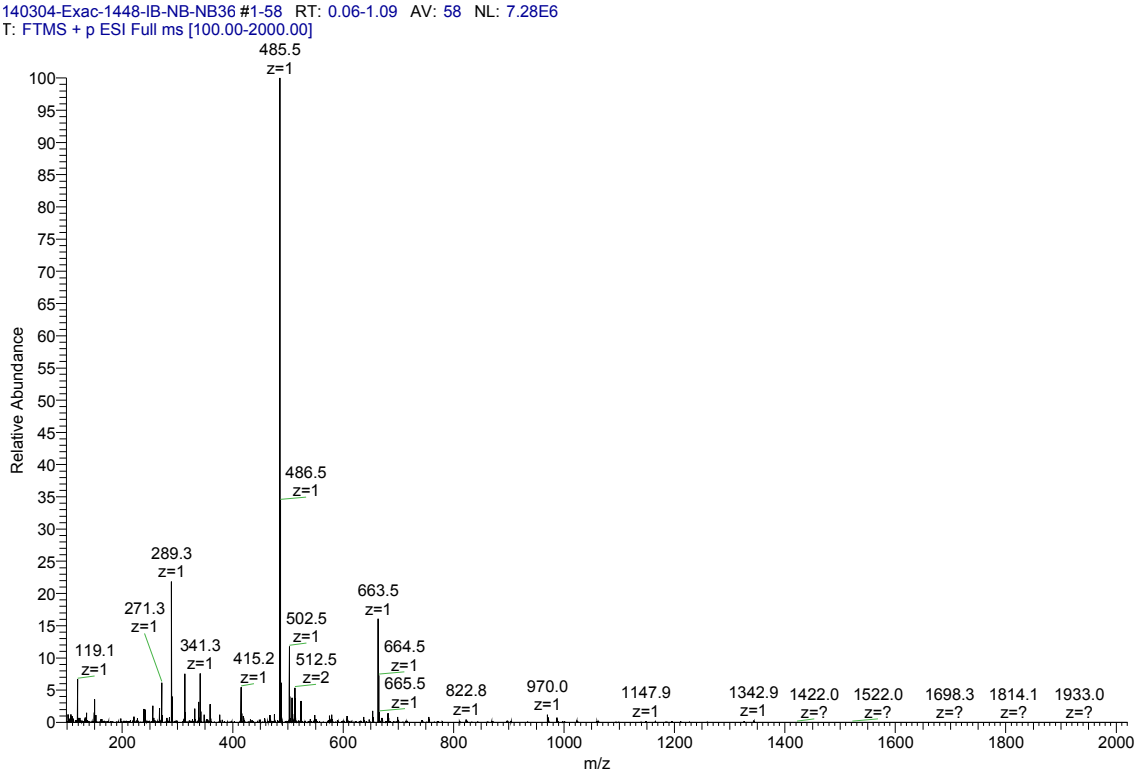

Figure S8. ESI-MS spectrum of compound **8.**

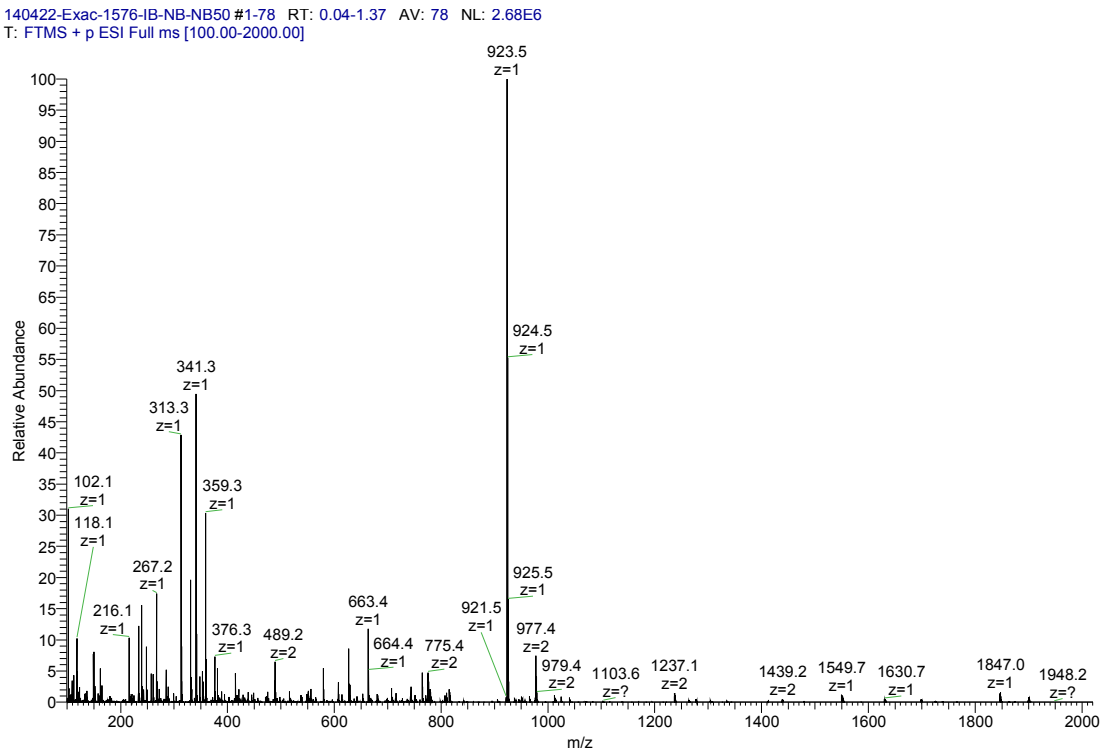

Figure S9. ESI-MS spectrum of RfdiC14 (compound **10**).

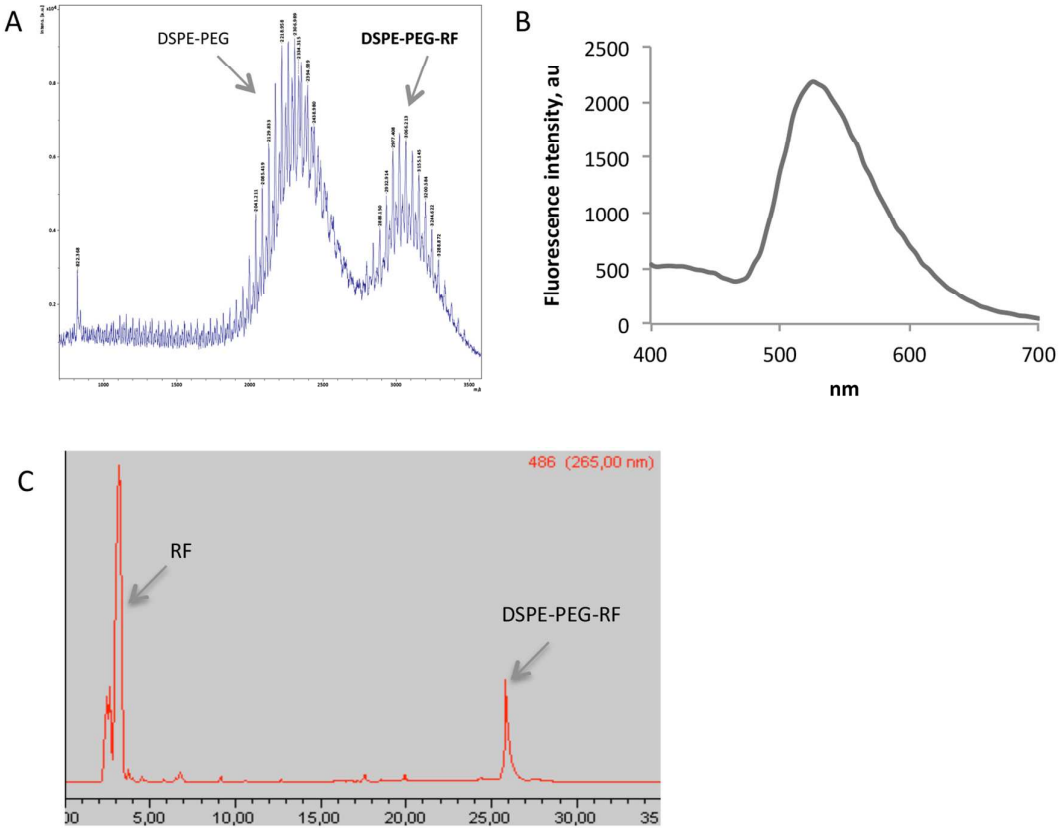

Figure S10. Characterization of compound 11 (DSPE-PEG-RF): A. MALDI mass spectrum of DSPE-PEG-RF; B. Fluorescence emission spectrum of DSPE-PEG-RF; C. Reverse-phase HPLC chromatogram of DSPE-PEG-RF synthesis.

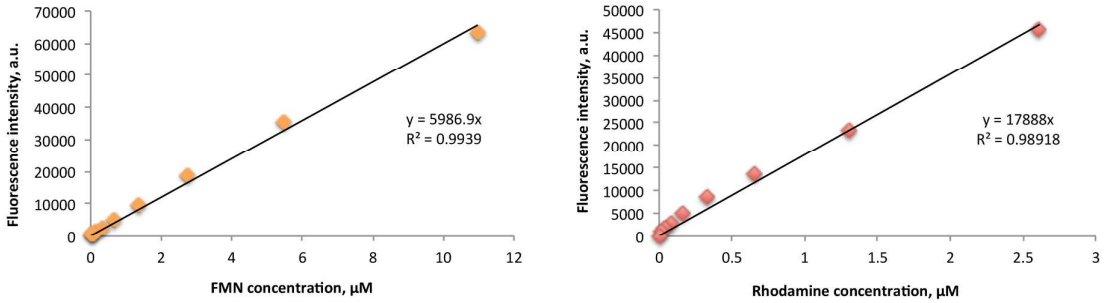

Figure S11. Calibration curves for riboflavin (*left*) and rhodamine B (*right*) in buffer.

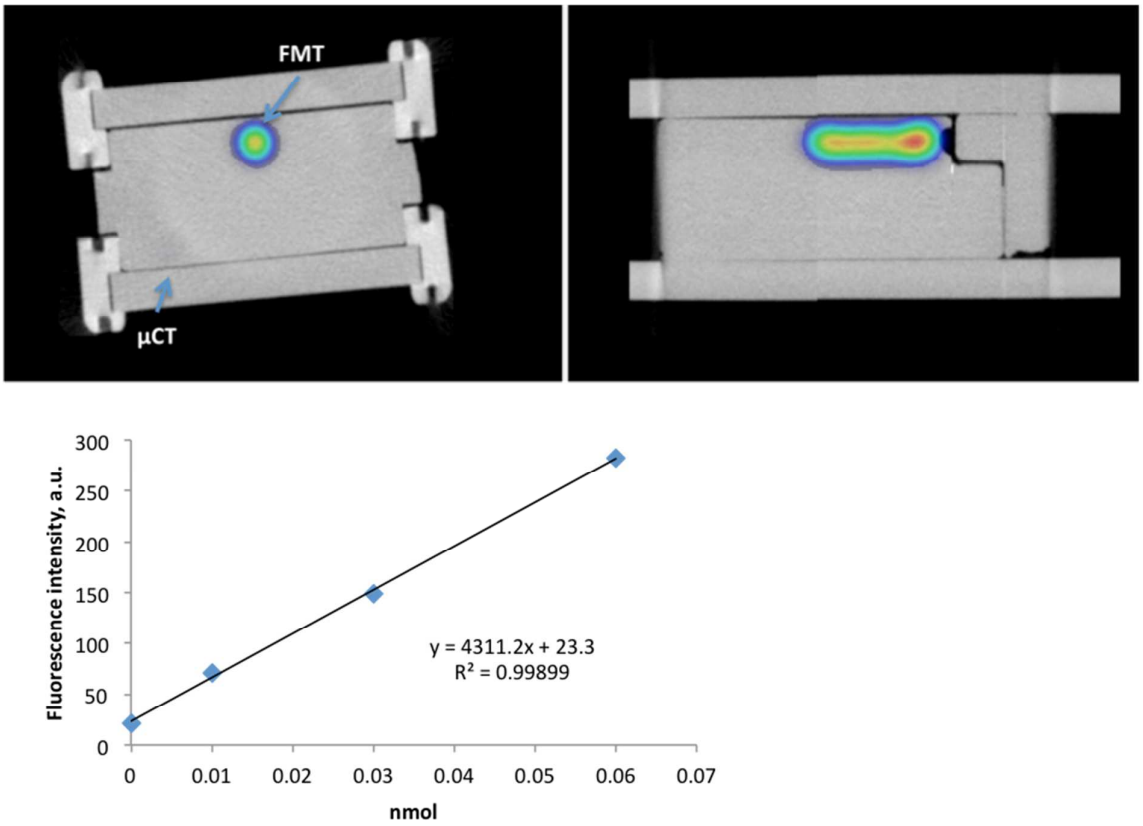

Figure S12. Up and side view of phantom image obtained from μCT and FMT fusion (up); μCT/FMT study of DiR liposomes in phantom, fluorescence (ex. 750 nm) signal intensities are plotted against DiR liposomes quantity (nmol) (*down*). The linear dependence between DiR labelled LCL and the emitted fluorescence, described by the following equation - y = 4311.2x + 23.3 (R^2 = 0.99238), where y represents the fluorescence signal intensity and x – the quantity of DiR in nmol.

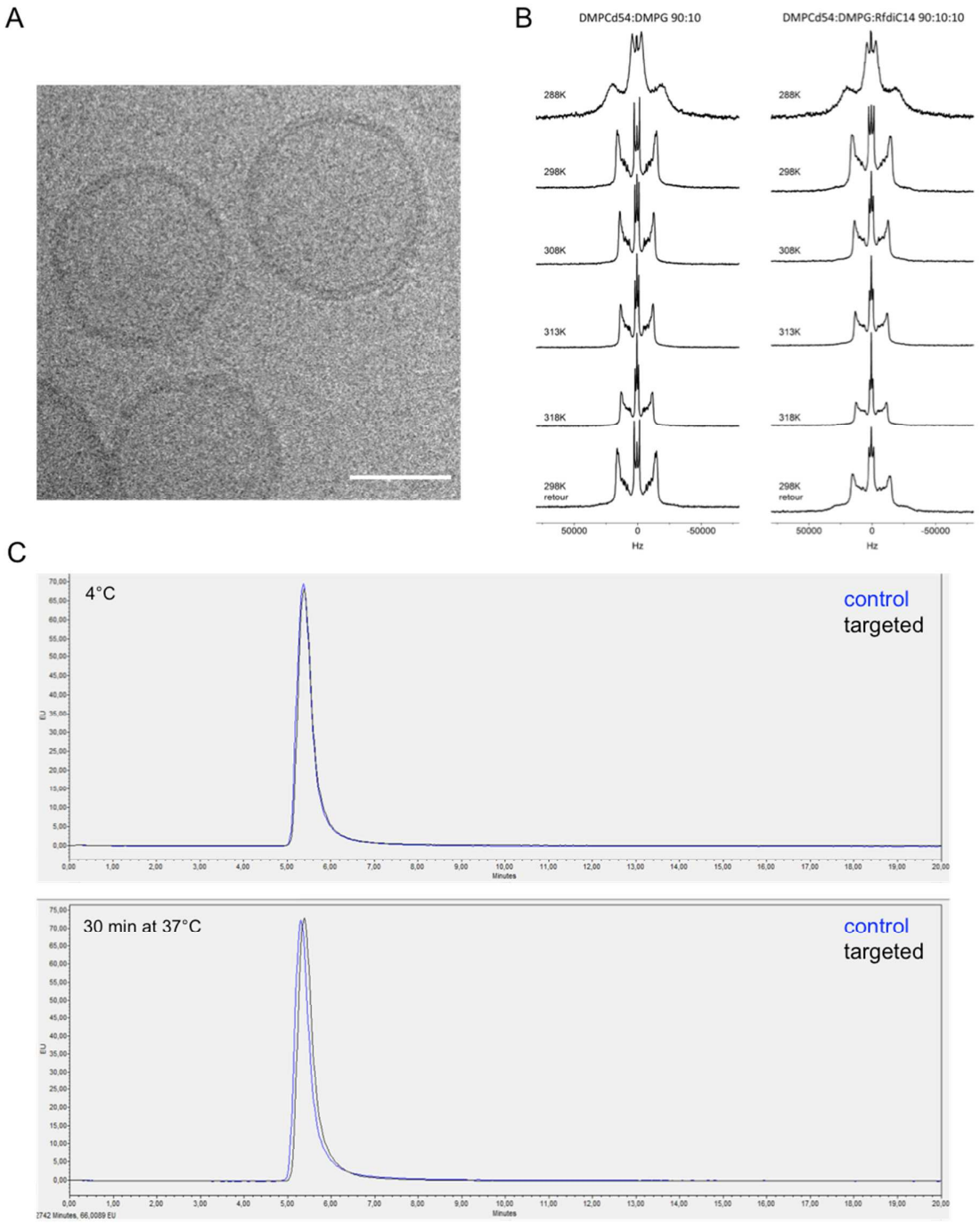

Figure S13. Morphology and stability characterization of control and targeted liposomes: A. Cryo-EM photograph of targeted liposomes; scale bar 50 nm. B. ^{2}H-NMR spectra of DMPC-d54: DMPG (left) and DMPCd54:DMPG:RfdiC14 (right); C. GPC profile of control and targeted liposomes at storage conditions (4°C) and after 30 min heating at 37°C, control formulation is depicted in blue and targeted is in black.

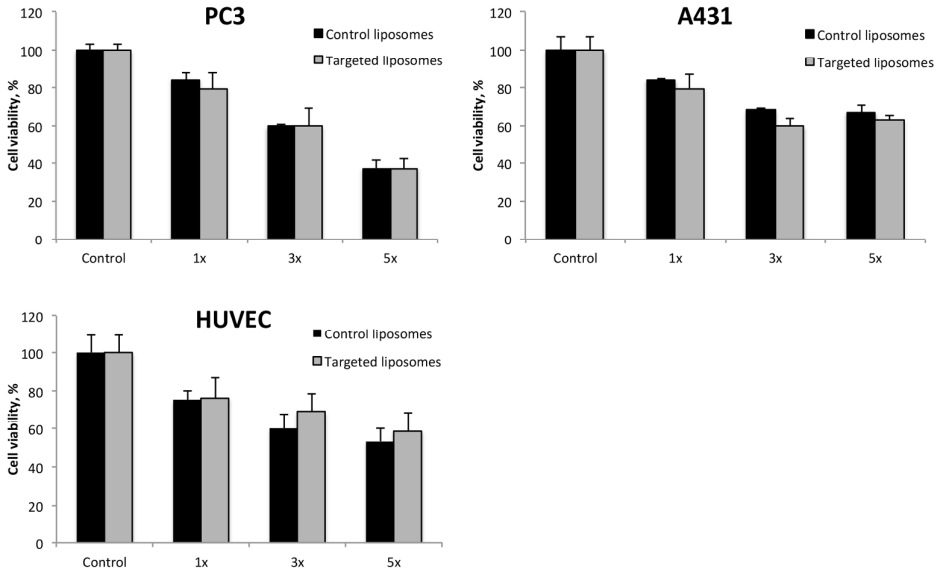

Figure S14. MTT cytotoxicity assay results. PC3 and A431 cells as well as HUVEC were incubated with standard (50 nM or 1x) and higher concentration (150 nM and 250 nM for 3x and 5x, respectively) of targeted and control liposomes; the values are presented as mean ± SD from n=3 experiments.

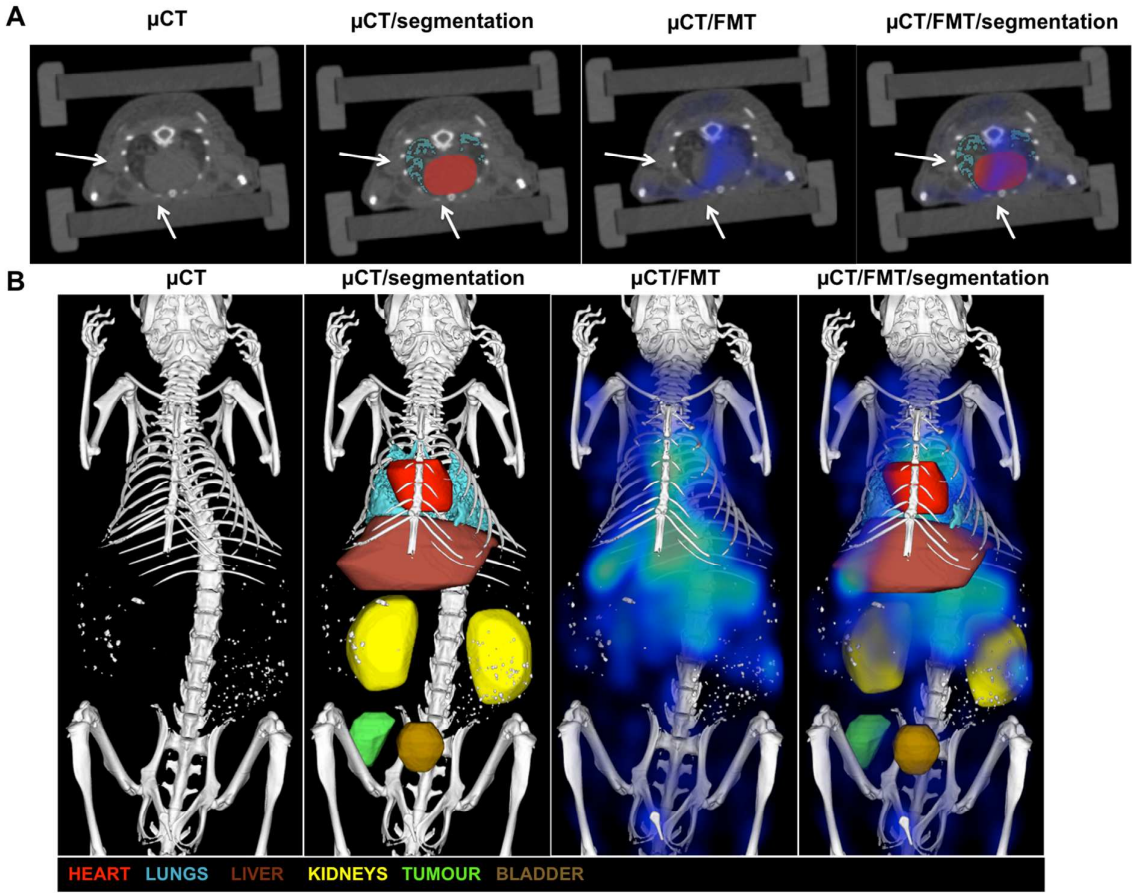

Figure S15. A. Various steps of organ segmentation in transverse view of a mouse; heart (red) and lungs (light blue) are marked with white arrows. µCT contrast is grey and fluorescent signal appears in a shape of dark blue cloud; B. Various steps of organ reconstruction and fluorescence quantification in 3D. Segmented organs are presented in various colours: heart – red, lungs – light blue, liver – brown, kidneys – yellow, tumour – green, bladder – beige. Fluorescent signal appears in the form of diffuse blue clouds.

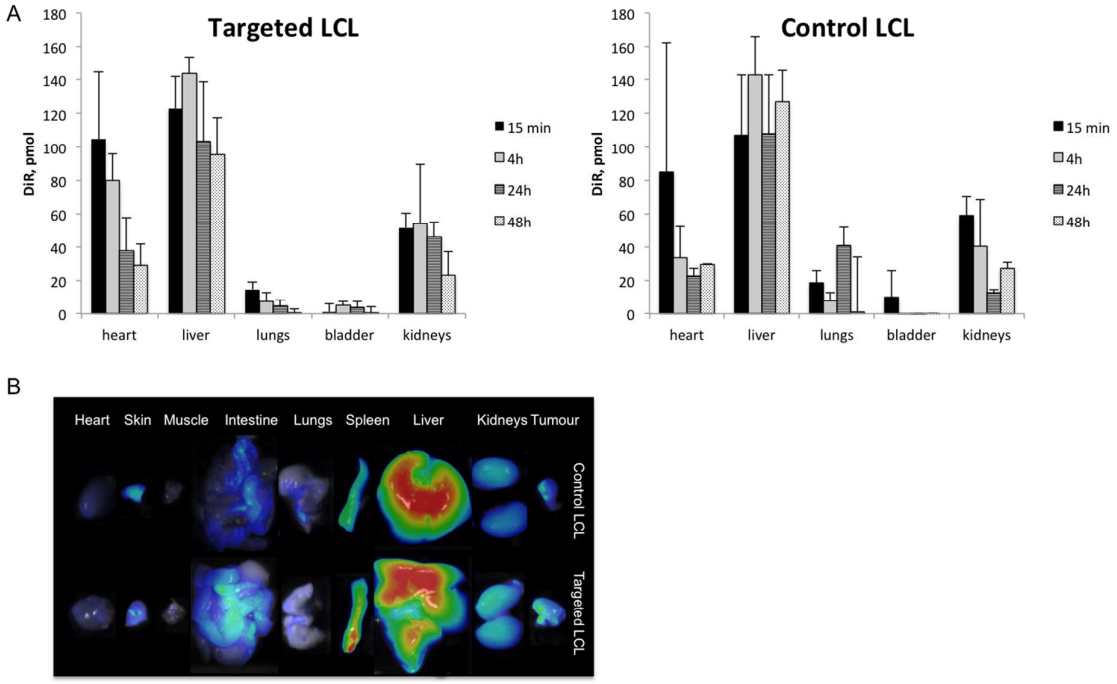

Figure S16. Biodistribution of LCL *in vivo*: A. Longitudinal 3D fluorescence quantification in healthy organs after i.v. injection of control or targeted LCL; B. *ex vivo* 2D fluorescence reflectance images of various organs and PC3 tumour xenografts from control and targeted group. Results presented as average ± SD from n=3 mice per group, SD – standard deviation.